S E S 2 0 1 1
Seventh Scientific Conference with International Participation
SPACE, ECOLOGY, SAFETY
29 November – 1 December 2011, Sofia, Bulgaria

THE AURORAL 5577 Å AND 6300 Å EMISSIONS DURING SUBSTORMS

Veneta Guineva[1], Irina Despirak[2], Rolf Werner[1]

[1]Space Research and Technology Institute – Bulgarian Academy of Sciences
[2]Polar Geophysical Institute, RAS, Apatity, Murmansk region, 184200, Russia
e-mail: v_guineva@yahoo.com

Keywords: *Aurora emissions, substorms, auroral bulge, polar edge boundaries.*

Abstract: *The 5577 Å and 6300 Å emissions intensities have been studied during substorms development. The emissions intensities in front of the polar edge of the auroral bulge, in the polar edge and inside it have been compared and estimations about the nature of the particle precipitation spectra in these regions have been made.*

Data from two All-Sky Imagers: at Andenes (69.3°N, 16.03°E) and at Longyearbyen, Svalbard (78.20°N, 15.83°E), Norway from 2005-2006 observations have been used. The interplanetary conditions have been determined by WIND satellite data. The substorm development has been followed up by the magnetic field components data from the IMAGE magnetometer network. Different methods to determine the boundaries of the polar edge of the substorm auroral bulge are examined. A simple threshold method is applied (in our case an increase of the 5577 Å emission intensity above its mean value by 1σ - least square deviation). The boundaries of the bulge polar edge were evaluated and analyzed by Chow test, as well. The obtained by both methods boundaries coincide very well.

АВРОРАЛНИТЕ ЕМИСИИ 5577 Å И 6300 Å ПО ВРЕМЕ НА СУББУРИ

Венета Гинева[1], Ирина Деспирак[2], Ролф Вернер[1]

[1]Институт за космически изследвания и технологии – Българска академия на науките
[2]Полярен геофизически институт, РАН, Апатити, Мурманска област, 184200, Русия
e-mail: v_guineva@yahoo.com

Ключови думи: *аврорални емисии,суббури, аврорална изпъкналост, граници на полярния край на авроралната изпъкналост.*

Абстракт: *Изследвани са интензивностите на емисиите 5577 Å и 6300 Å при развитие на суббури. Сравнени са интензивностите на емисиите преди полярния край на авроралната изпъкналост, в полярния край на изпъкналостта и вътре в нея и е направена преценка на характера на спектъра на изсипващите се частици в тези области.*

Използвани са данни от две all-sky камери: в Анденес, (69.3°N, 16.03°E) и Лонгиербиен, Шпицберген (78.20°N, 15.83°E), Норвегия, от наблюдения през 2005-2006 г. Междупланетните условия се определят по данни от спътника WIND. Развитието на суббурите е проследено по данни за компонентите на магнитното поле от мрежата магнитометри IMAGE. Разгледани са различни методи за определяне на границите на полярния край на суббуревата аврорална изпъкналост. Приложен е прост метод с използване на праг (в случая нарастване на интензивността на емисията 5577 Å над средната й стойност с 1σ - средно квадратично отклонение). Границите на полярния край на изпъкналостта са определени и анализирани чрез Chow тест. Получените по двата метода граници съвпадат много добре.

Introduction

Substorms are a particular phenomenon, related to a number of processes in the magnetosphere and ionosphere, summarized by Akasofu [1]. It was established that the substorm development goes on in the following way: the substorm expansion phase begins with the flash of one arc, usually the most equatorial one between the existing discrete auroral arcs. After this the area occupied by bright, short-lived arcs – the auroral bulge – is expanding in all directions, mainly toward

the pole, to the West and to the East [2, 3]. At the time of maximal stage of substorm development the auroral bulge reaches its greatest width and occupies a maximum area. Further, during the recovery phase, the auroral bulge begins to shrink, its polar edge moves to the equator and, the South one – to the pole, the bright discrete arcs degenerate into irregular strips and fade [4, 5].

The emissions 5577 Å and 6300 Å of the atomic oxygen are among the most prominent auroral emissions. They result from forbidden OI transitions. The oxygen green line 5577 Å is emitted by $O(^1S)$ atoms with radiative lifetime 1 s. The red line 6300 Å is part from the doublet 6300/6364 Å, originating from the $O(^1D)$ state, only 2 eV above the ground state of O. The $O(^1D)$ state is metastable, with radiative lifetime about 100s. [6]. The auroral optical emissions are observed at altitudes above 100 km and generate from precipitating particles with energies <15 keV [7]. The intensity of the separate optical emissions is related to the energy and flux of precipitating electrons in the corresponding energy band. The 5577 Å intensity depends on the average fluxes in 108-120 km height range (2-7 keV energy range) [8], and the 6300 Å intensity – to the average fluxes in the 180-250 km height range (5.10^{-3} – 5 eV energy range). The change of the ratio $I_{6300Å}/I_{5577Å}$ is an indicator of the changes in the precipitating energy distribution. The intensity ratios can be used to estimate the characteristic energy of the precipitating auroral particles and even to study the atmosphere composition changes due to auroral precipitation [9].

Auroras observations have always played a fundamental role for the study of the solar wind-magnetosphere-ionosphere interaction during substorms. The auroral emissions behaviour during substorms is the result of a chain of subsequent phenomena connected to energy releases and changes in the near-Earth magnetospheric tail regions. Therefore the study of the auroral arcs and smaller structures gives information about the transfer of energy and momentum between these regions [10]. To clarify the processes running during substorms, the examination of the emissions behaviour in different regions, in particular at the polar edge of the auroral bulge and inside it. For that reason the boundaries of these regions have to be defined. Such definitions are not suggested. It was established that discrete auroral emissions occur at the poleward edge of the bulge [2] that corresponds to higher energy particles and brighter emissions. But there are only a few works in which energy particles in auroras at the polar edge and inside the auroral bulge are compared. For example, such a work, in which the dynamics of the polar boundary of the auroral oval during substorm on the basis of all-sky camera and spectrograph observations in Mirniy observatory was studied in the work by Zverev and Starkov [11]. It was shown that more energetic particles are observed at the polar edge of the luminosity band.

In this work we present studies to determine the boundaries of the polar edge of the auroral bulge and we submit methods and criteria to specify them. In the work All-Sky Imagers data are presented, revealing the substorm development as it was seen in the auroras displays. We consider the variations of auroral emissions at the polar edge of the auroral bulge and inside the bulge.

Data used

For the study, data from 2 all-sky imagers (ASI) are used. The all-sky imagers are positioned at Andøya Rocket Range (ARR), Andenes (AND) (69.3°N, 16.03°E) and in the Auroral Observatory, Longyearbyen, Svalbard (LYR) (78.20°N, 15.83°E). Both devices are identical. The all-sky imagers have 180° field of view. The used CCD cameras are monochromatic, 512x512 pixels, with 16-bit intensity resolution and up to 10 s time resolution. The 5577 Å and 6300 Å emissions are recorded automatically with 10 s time resolution. The raw images are accumulated at the Oslo University.

Data by IMAGE magnetometers network are used to verify substorm presence, substorm onset time and further development. The timing of negative H-bays is an established substorm indicator [3] and substantiates the identification and development of substorms.

Data from WIND satellite are used to monitor the interplanetary conditions.

We used the criteria for data selection listed in [14]. Measurements of the ASI at Andenes and Longyearbyen from the 2005-2006 observational season were used for the study.

Data processing

A part of the AND raw images (512x512 pixels) is taken in such a way that they are centered at the station and a field of view of ±70˚ is obtained. Data interpolation is performed to obtain the intensities in 467x467 equidistant points. Thus, a space angle resolution of 0.3˚ near zenith is obtained. But the image pixels, calculated this way, are not situated at the same distance from each other. In order to get a better notion of the real pixel locations, the images are projected on the geographic map. The latitude/longitude set and the continental borders are plotted. An image section is used to obtain a circle area corresponding to ±70˚ field of view of the all-sky imager. In the purpose to obtain better pictures, in which the emerging or passing features are well seen in a number of

cases, using the same scale, ln(I(counts)) is drawn in the images. The location of the station magnetic zenith is marked by a black point (such processed images are presented in Fig.1).

LYR raw images are processed the same way. There a field of view of ±75° is cut and a resolution of 0.35° near zenith is obtained.

To follow the time development of the intensities, we have examined the intensities of both lines in geomagnetic zenith of the station. The geographic and geomagnetic coordinates of the data points have been computed for heights 120 km for the 5577 Å emission and 250 km for the 6300 Å one. To construct the course of the emissions intensities and their ratio, we are using the data point of each image, corresponding to the station geomagnetic zenith. The obtained series are interpolated in order to obtain equidistant points, coinciding for 5577 Å and 6300 Å luminosity.

Unfortunately, the time dependence of the zenith intensity cannot give information about its spatial configuration. For example, looking only the course plots, we can't know if a feature, present there, is an arc, and if so, whether this arc is moving over the station, or is generated there and fade without moving. That is why we are examining both, the consecutive images and the corresponding time dependences.

Methods of determining the boundaries of auroral zone structures

The simplest and widespread method to determine the boundaries of a structure in the emissions intensity distribution is some threshold method. The place or the moment when the intensity reaches this threshold represents the searched boundary, and the intensity values above the threshold belong to the examined structure. This way the boundaries of one-dimensional as well as two-dimensional distributions are determined. Different variants to determine the threshold exist. Usually its value is higher than the mean intensity in the observed region. In the past, the sum of the mean value plus a part of the maximal value, for example 10% of the maximal structure intensity was used [12]. In consequence of the fast development of the computer technologies and the possibility of fast fulfillment of a lot of computations as additional value to the mean one was assumed the standard deviation σ. At present the most common threshold is the mean value + 1σ [e.g. 13, 14]. The standard deviation is given by:

(1) $$\sigma = \sqrt{\frac{\sum_{i=1}^{n}(x_i - \bar{x})^2}{n}},$$

where

(2) $$\bar{x} = \frac{1}{n}\sum_{i=1}^{n} x_i ,$$

and *n* is the values number. So the threshold intensity value is:

(3) $$I_{threshold} = \bar{x} + \sigma$$

The boundary between two regions – "calm" glow and "structure" (which can be an arc or any other structure) can be determined by Chow test [15] as well. Chow test is a statistical and econometric test about that if the coefficients of two linear regressions of different data sets are equal. In econometrics the Chow test is mostly used to analyse time series in order to determine structural breaks or changes. Let us examine two groups of data, N_1 and N_2 in number, respectively. If *S* is the sum of the squared residuals from the combined data $n=N_1+N_2$: $S = \sum_{i=1}^{n}(x_i - \bar{x})^2$, S_1 and S_2 are the sums of the squared residuals from the first and second group, respectively: $S_1 = \sum_{i=1}^{N_1}(x_i - \bar{x})^2$, $S_2 = \sum_{i=1}^{N_2}(x_i - \bar{x})^2$, then the Chow test statistic is:

(4) $$\frac{(S - (S_1 + S_2))/(k)}{(S_1 + S_2)/(N_1 + N_2 - 2k)}$$

This test statistic follows the F distribution with *k* parameters and *(n-2k)* degrees of freedom.

Determination of the boundaries of the polar edge of the auroral bulge

The polar edge represents a dynamic band in the North part of the substorm bulge, as it was noted by Zverev and Starkov [11]. This band comprises the arc flashed first during the substorm beginning (usually the brightest one). The polar edge of the substorm bulge moves fast to the pole, its form and dimensions, as well as the emissions intensities inside it changing meanwhile in time scales of the order of seconds.

To determine the polar edge boundaries, the consecutive intensity distributions and the course of the 5577 Å emission in magnetic zenith have been used. In Fig.1 the development of a substorm over Andenes on 3.11.2005 is shown. Chosen two-dimensional distributions of 5577 Å emission intensity are presented, projected on the geographic map. The universal time is written in the upper part of every image. The geomagnetic zenith is marked by a black dot. In the upper row, the development, the movement of the polar edge of the bulge to the station and its passage over the zenith can be seen. In the bottom row, some arcs and other structures, generated or moving over zenith or near it inside the auroral bulge are shown.

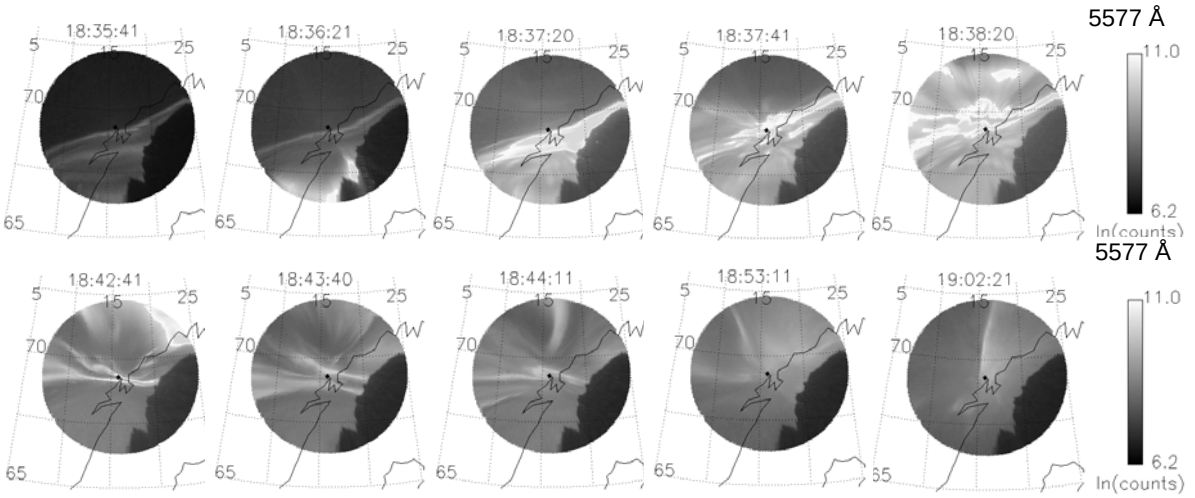

Fig.1. Chosen images of 5577 Å distributions by Andenes ASI during the development of a substorm on 3 November 2005. The upper row shows the substorm appearance in the field of view, the movement of the polar edge of the auroral bulge to the station geomagnetic zenith, and its overpassing. The bottom row presents some arcs and other structures in the auroral bulge appeared in zenith or near it.

Fig. 2 shows a part of the course of 5577 Å and 6300 Å emissions intensities in zenith, including the polar edge of the auroral bulge. The boundaries of the polar edge of the bulge are determined by the described above simple threshold method by the green emission development. The mean value was obtained for 2-3 hours measurements (700-1000 points), including the longest possible time interval before the substorm onset and the time of the substorm itself. The calculated threshold for this substorm is 8500 counts/sec. It is presented in Fig.2 by a dotted line. The polar edge boundaries are obtained in 18:37:30 UT and in 18:39:50 UT. But by examining the consecutive images it was found out that after its passage over zenith, the green arc of the polar edge broadened strongly, and in 18:38:41 UT crumbled away into many finer structures, arcs and rays. The polar edge of the bulge was already to the North, still in the field of view. A new arc fleshed there in 18:39:20 UT. The intensity sharply decreased, but the whole field of view stayed illuminated and the intensity was higher than the threshold. The red arc followed the same behaviour and broke down in 18:38:02 UT. So, we took the polar edge boundaries in 18:37:30 UT and 18:38:02 UT.

To determine the boundaries of the polar edge of the auroral bulge by Chow test, the test is applied for one parameter – the green emission 5577 Å. Then

$$F(1, n-2) = \frac{(S - S_1 - S_2)(n-2)}{S_1 + S_2} \tag{5}$$

For the *F* distribution we have

$$F(1, \infty, 0.95) = 254 \tag{6}$$

Both examined regions differ by their structure, if the obtained values of *F* are greater than 254, and the precise boundary between the regions coincides with the *F* maximum. As an example, we present the application of the Chow test for the substorm on 3.11.2005 observed above Andenes in 18:37 UT. When choosing the interval containing two regions between which we will search a

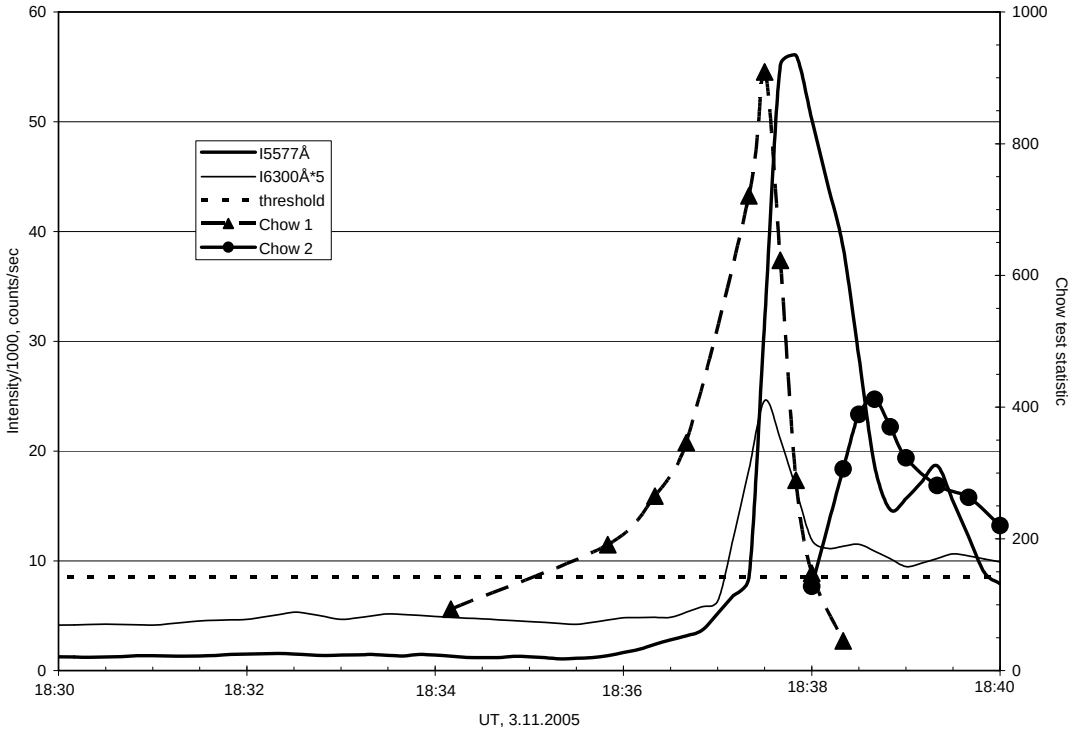

Fig. 2. Course of the 5577 Å and 6300 Å emissions intensities in the region of the polar edge of the auroral bulge during the substorm on 3.11.2005 in the geomagnetic zenith of Andenes station. The computed threshold is marked by a dotted line. The calculated values of the Chow test statistic to determine both boundaries of the polar edge of the bulge are plotted in the graph, connected by different lines. The triangles stand for the North boundary (Chow1) and the points – for the South one (Chow2). The maxima of the obtained dependences indicate the polar edge boundaries according to the Chow test.

boundary, several considerations have to be taken in mind: first, it is better to take an interval as long as possible, but on the other hand, the interval must cover two different regions, and not for example two regions, one of which include different structural elements.

For the determination of the North boundary of the polar edge of the auroral bulge the regions are the comparatively undisturbed glow before the substorm and the polar edge itself. These two regions are radically different and the boundary between them should be clearly outlined. For the common interval we don't take the values from the beginning of the measurements in 16:00 UT because some enhanced activity is observed about 17:20 UT, which could twist the result. Therefore we take the measurements from 18:00 UT to 18:38:02 UT, the moment determined as polar edge boundary by the used threshold method. The number of the data in this interval is n = 229, and the degrees of freedom are 227. After the implemented calculations and comparisons a maximal value of F = 909 at data number 921 which corresponds to 18:37:30 UT and 5577 Å intensity of 31.8 counts/sec. The obtained Chow test statistics (F-values) are presented in Fig.2. by triangles. By the threshold method the boundary is obtained at 8.5×10^3 counts/sec., which is just in 18:37:30 UT for the North boundary of the polar edge of the substorm bulge. Then for the first time an intensity value above the threshold is registered. The boundaries, obtained by both methods, completely coincide.

The determination of the South boundary of the polar edge of the auroral bulge involves the study of an interval, including the polar edge of the bulge and the measurements inside the auroral bulge. The determination of this boundary appears more complex because both regions don't differ so much, inside the bulge there are arcs, although not so intensive as the polar edge. For our case we examine the time interval from 18:37:30 UT, which is the defined by both methods North boundary of the polar edge of the bulge, to 19:26:41 UT, as long as we assume that the station zenith is inside the bulge. The number of the data in this interval is 287, and the degrees of freedom are 285. The Chow test statistic study leads to s maximal value F=412 for data number 927, in 18:38:30 UT. The obtained F values are presented in Fig.2 as points. By the threshold method this boundary is obtained in 18:39:50 UT, but after the described above examinations the South boundary position is accepted in 18:38:02 UT. The obtained by both methods boundaries are close to each other. It appears that in this case the South boundary of the polar edge of the bulge is determined more accurately by Chow test, whereas using the threshold method an error would be made if only the intensity course in zenith is observed and the overall spatial development isn't taken into account.

Conclusions

A definition of the polar edge as a dynamic band in the North part of the auroral bulge comprising the brightest arc fleshed first during the substorm onset is assumed.

Criteria to define the boundaries of the polar edge of the auroral bulge by optical measurements are submitted. Two methods are applied: a threshold method and Chow test method. The boundaries determined by both methods coincide very well. The polar edge boundaries of the auroral bulge can be determined by these methods when studies of the substorm bulge are carried out.

Acknowledgements

Data access has been provided under the Project “ALOMAR eARI” (RITA-CT-2003-506208), Andenes, Norway. This Project received research funding from the EC’s 6th Framework Program.

We are grateful to E. Trøndsen and the University of Oslo, Department of Physics, Oslo, Norway for providing data from the All-Sky Imagers at Andenes and Longyearbyen and for computing the geographic coordinates of both image matrices and to Dr. S. Marple and the Department of Communications Systems at Lancaster University (UK) for the transform of the geographic coordinates of the image matrices in geomagnetic ones.

The study is part of a joint Russian -Bulgarian project “The influence of solar activity and solar wind streams on the magnetospheric disturbances, particle precipitations and auroral emissions” of PGI RAS and STIL-BAS under the program for fundamental space research between RAS and BAS.

References:

1. A k a s o f u, S.-I., 2004. Several ‘controversial’ issues on substorms. *Space Sci. Rev.,* 113, pp.1-40.
2. A k a s o f u, S.-I., 1964. The development of the auroral substorm. *Planet. Space Sci.,* 12, pp.273-282.
3. A k a s o f u, S.-I., 1965. Dynamic morpholody of auroras. *Space Sci. Rev.*, 4, pp.498-540.
4. S t a r k o v, G. V., Ya. I. F e l d s h t e I n, 1971. Substorms in the polar auroras. *Geomagnetism and aeronomy*, 11, pp.560-562.
5. I s a e v, S. I., M. I. P u d o v k i n, 1972. Polar aurora and processes in Earth magnetosphere (Ed. OL, A.I., Moskow: Nauka).
6. R e e s, M.H., D. L u c k e y, 1974. Auroral electron energy derived from ratio of spectroscopic emissions 1. Model computations. *J. Geophys. Res.* 79, pp.5181-5185.
7. K o s c h, M. J., F. H o n a r y, C. F. d e l P o z o, and S.R. M a r p l e, 2001. High-resolution maps of the characteristic energy of precipitating auroral particles. *J. Geophys. Res.* 106(A12), 28925-28937.
8. D e l P o z o, C. F., M. J. K o s c h, and F. H o n a r y, 2002. Estimation of the characteristic energy of electron precipitation. *Ann. Geophys.* 20, pp.1349-1359.
9. H e c h t, J. H., D. J. S t r i c k l a n d, M. G. C o n d e, 2006. The application of ground-based optical techniques for inferring electron energy deposition and composition change during auroral precipitation events. *J. Atm. Sol.-Terr. Phys.* 68, pp.1502–1519.
10. F r e y, H.U., O. A m m, C. C. C h a s t o n, S. F u, G. H a e r e n d e l, L. J u u s o l a, T. K a r l s s o n, B. L a n c h e s t e r, R. N a k a m u r a, N. Ø s t g a a r d, T. S a k a n o i, E. S é r a n, D. W h I t e r, J. W e y g a n d, K. A s a m u r a, M. H I r a h a r a, 2010. Small and meso-scale properties of a substorm onset auroral arc. *J. Geophys. Res.* 115, A10209, doi:10.1029/2010JA015537.
11. Z v e r e v, V. L., and G. V. S t a r k o v, 1972. Dynamic of polar boundary of aurora oval in process of auroral substorm development. in: *Sbornik Antarktika*, The USSR Academy of Sciences, Nauka, Moskva, 11, pp.29-40.
12. G o g o s h e v, M. M., G. G. S h e p h e r d, P. V. M a g l o v a, V. Chr. G u i n e v a and Ts. P. D a t c h e v, 1987. Structure of the Polar Oval from Simultaneous Observations of the Optical Emissions and Particle Precipitations During the Period of High Solar Activity 1981 - 1982, *Adv. Space Res.*, 7, pp.(8)7 - (8)10.
13. C o n s o l i n i, G., E. P. B a l s a m o, M. C a n d i d i, P. D e M i c h e l i s, M. F. M a r c u c c i, and L. M o r l c i, 2009. Auroral observations at the Mario Zucchelli Base (Antarctica). Morphological features. *Mem. S. A. It.* 80, pp.268-269.
14. G u i n e v a, V., I. D e s p i r a k, E. T r ø n d s e n, R. W e r n e r, 2011. Peculiarities of the auroral emissions during substorms associated with high-speed solar wind streams, *Opt. Pura Apl.,* 44(4), pp.617-622.
15. C h o w, G. C., 1960. Tests of Equality Between Sets of Coefficients in Two Linear Regressions. *Econom.* 28 (3), pp.591–605.